J Comput Aided Mol Des (2014) 28:123–134
DOI 10.1007/s10822-014-9737-z

Reinforcing the membrane-mediated mechanism of action of the anti-tuberculosis candidate drug thioridazine with molecular simulations

Wojciech Kopec · Himanshu Khandelia

Received: 13 November 2013 / Accepted: 19 February 2014 / Published online: 1 March 2014

Abstract Thioridazine is a well-known dopamine-antagonist drug with a wide range of pharmacological properties ranging from neuroleptic to antimicrobial and even anticancer activity. Thioridazine is a critical component of a promising multi-drug therapy against *M. tuberculosis*. Amongst the various proposed mechanisms of action, the cell membrane-mediated one is peculiarly tempting due to the distinctive feature of phenothiazine drug family to accumulate in selected body tissues. In this study, we employ long-scale molecular dynamics simulations to investigate the interactions of three different concentrations of thioridazine with zwitterionic and negatively charged model lipid membranes. Thioridazine partitions into the interfacial region of membranes and modifies their structural and dynamic properties, however dissimilarly so at the highest membrane-occurring concentration, that appears to be obtainable only for the negatively charged bilayer. We show that the origin of such changes is the drug induced decrease of the interfacial tension, which ultimately leads to the significant membrane expansion. Our findings support the hypothesis that the phenothiazines therapeutic activity may arise from the drug–membrane interactions, and reinforce the wider, emerging view of action of many small, bioactive compounds.

Keywords Antipsychotics · Molecular dynamics · Lipid bilayer · Drug–membrane interactions · *M. tuberculosis*

Introduction

The interactions of small molecules with lipid membranes and their impact on the membrane properties play an essential role in many biophysical phenomena [1]. Usually driven by weak, non-bonded interactions, partitioning of host molecules (drugs) in bilayers is important not only in the context of their cellular bioavailability, but also in explaining a therapeutic activity of some types of drugs. Classically, drugs target biopolymers—proteins and nucleic acids [2]. However, it has been postulated that several classes of drugs may exert their pharmacological effects by influencing the lipid bilayer properties [3–5], such as fluidity, thickness or membrane electrostatic potential, which may subsequently affect trans-membrane proteins. For example, changes in a membrane thickness and/or curvature can cause a hydrophobic mismatch, a situation when the hydrophobic length of the protein embedded in the membrane does not match the length of the membrane hydrophobic core [6]. Such unfavorable situations may trigger a conformational transition of the protein, thus modulating its function [7]. Drug dissolution in lipids, first observed by Meyer and Overton for anesthetics, was later proposed as an important step in the targeting trans-membrane proteins where binding to the protein occurs from the surrounding lipid membrane. In a modern theory of general anesthesia, drug molecules alter the conformations of ion channels by changing the membrane lateral pressure profile (LPP) in the membrane [8, 9], and thereby modulate ion transport. Interestingly, the location of the ligand-gated ion channel (LGIC) binding site, targeted by general anesthetic

Electronic supplementary material The online version of this article (doi:10.1007/s10822-014-9737-z) contains supplementary material, which is available to authorized users.

W. Kopec · H. Khandelia (✉)
MEMPHYS - Center for Biomembrane Physics, University of Southern Denmark, Campusvej 55, 5230 Odense M, Denmark
e-mail: hkhandelia@gmail.com; hkhandel@memphys.sdu.dk
URL: http://www.memphys.sdu.dk/~hkhandel/

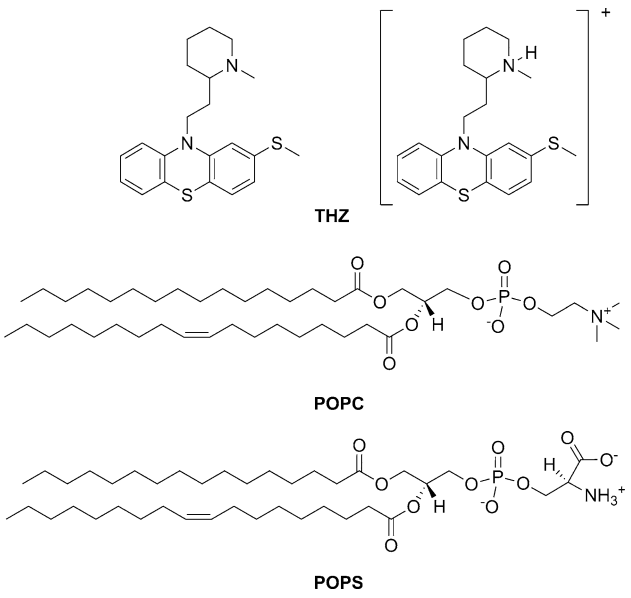

Fig. 1 Chemical formulas of THZ in its neutral and charged form, as well as simulated lipid species

propofol, coincides with the depth of the drug immersion inside the membrane [10]. Such mechanisms, which are different from the canonical view of high-affinity drug-protein binding, are especially appealing for drugs that exhibit a wide range of therapeutic activities, which cannot originate from binding to a single molecular target. There is experimental evidence that some of these effects might be indeed membrane-mediated [11–13].

Thioridazine (10-{2-[(*RS*)-1-methylpiperidin-2-yl]ethyl}-2-methylsulfanylphenothiazine, THZ, Fig. 1), an old neuroleptic drug, has recently reclaimed the attention of the scientific community.

Together with other phenothiazines, such as chlorpromazine, THZ was extensively used against psychotic disorders like schizophrenia and psychosis [14, 15]. Unfortunately, the phenothiazines might cause severe side effects, and are no longer commonly prescribed [15]. However, after years of omission from the clinic, THZ has emerged as a very promising candidate for anticancer, antimicrobial, and most significantly, for its property of inducing antibiotic resistance reversal in particularly refractory multi-drug-resistant strains of *M. tuberculosis* [16], inexpensive drug.

THZ influences DNA metabolism of the bacterium cell [17, 18], inhibits its Ca^{2+} uptake [18, 19], inhibits bacterium efflux pumps, and alters the fluidity, thickness and lateral organization of the bacterial cell membrane [20]. The inhibition of the efflux pumps, that makes THZ an excellent choice for co-drug formulations, may originate from direct drug-protein binding, but might also be a consequence of the drug-induced perturbation of the lipid membrane. The concentration of drugs required to significantly alter the cell membrane properties usually exceeds the obtainable in vivo concentration [21]. However, the concentration of phenothiazines in pulmonary tissue is more than 100 times higher than the concentration in plasma [22]. Finally, Bhatia et al. [23] demonstrated that THZ selectively targets cancer stem cells that are thought to be a source and/or a sustaining agent of different malignancies and their metastatic behavior. Being an antipsychotic drug, THZ operates as an antagonist of transmembrane dopamine receptors [24], that are overexpressed by cancer stem cells of some cancers [25]. Thus, THZ is potentially an excellent marker in e.g. breast cancer and leukemia diagnosis. Recent evidence suggests that neurotransmitters, such as dopamine or serotonin, may exert the effect on their receptors via the synaptic membrane [26–28], and THZ may act similarly.

The exact mechanism of action of THZ remains unclear. Amongst the various possibilities, the interaction of THZ with lipid membranes may play a key role in its widespread therapeutic activity [29]. In this paper, we attempt to test this hypothesis. The precise description of the molecular mechanism will also shed some light on important biophysical issues such as membrane reorganization induced by host molecules, properties of doped membranes, and coexistence of lipids and other chemicals inside membranes. Chemically, THZ possesses a rigid, hydrophobic tricyclic group, connected with a piperidine ring (Fig. 1). Being partially planar and aromatic, it bears similarities to the prime regulator of biological membranes: cholesterol. The piperidine amino group may occur in different protonation states (pKa = 9.5) [30]. THZ is lipophilic [31] and cationic at neutral pH. Importantly, both enantiomeric forms of THZ are potent antibacterial agents. The levorotatory (−) form, which accumulates more in body tissues, and is more potent, fortunately has less neurological side-effects than the more harmful (+) form [32].

Here, we employ molecular dynamics (MD) simulations to follow the molecular motion of positively charged THZ near and inside the model lipid membranes, to describe the bilayer properties after THZ partitioning, in the concentration-depended manner, and to quantify specific interactions between THZ and lipid molecules. The overall goal is to investigate if THZ can alter bilayer properties to an extent significant enough to influence the action of transmembrane proteins. We use two different model bilayers—zwitterionic POPC (1-palmitoyl-2-oleoyl-sn-glycero-3-phosphocholine) and negatively charged, mixed POPC/POPS (1-palmitoyl-2-oleoyl-*sn*-glycero-3-phospho-L-serine) bilayer to evaluate the effect of membrane composition on the drug–lipid interactions.

We find that THZ interacts strongly with both types of membranes. The interactions are more pronounced with the

charged membrane. THZ acts as a membrane stabilizer at moderate membrane-concentrations, ordering the membrane. At higher concentration, however, its presence in the membrane leads to significant disorder and expansion of the bilayer. In the "Results" section, the interactions of THZ with lipid molecules are described. In the "Discussion" section we compare our results with previous simulations of similar compounds, and draw conclusions about possibly membrane-mediated mechanism of THZ. To our best knowledge, this is the first simulation report of the impact of THZ on lipid bilayers using long-scale MD simulations. Our results provide a compelling explanation of the membrane-mediated action of phenothiazines, described on the atomistic level.

Methods

Simulations of THZ with a zwitterionic POPC bilayer and negatively charged POPC/POPS bilayer (4:1 POPC:POPS molar ratio) were performed. The POPC bilayer contained 128 lipids, while the POPC/POPS bilayer contained 130 lipids. Three different THZ:lipid ratios were used—1:8, 1:4, 1:2. From now on, the systems containing POPC will be called POPCTHZ16, POPCTHZ32, POPCTHZ64, and systems also containing POPS will be labeled PCPSTHZ16, PCPSTHZ32, PCPSTHZ64, with the letters denoting the type of bilayer, and the number denoting the number of THZ molecules. Simulations of pure bilayers in the presence of pure water and required counterions were also carried out (hereafter referred to as POPC and PCPS). All systems were hydrated with approximately 9,100 water molecules ($\sim$70 water molecules per lipid) that provided the full membrane hydration. Detailed information about the performed simulations is provided in Table 1.

Force field parameters

The Berger united atom force field [33], with parameters adapted from http://moose.bio.ucalgary.ca/, was used for POPC and POPS. Dihedrals around the tail double bond were modified to better reproduce order parameters, as reported by Bachar et al. [34]. Water was represented by the single point charge (SPC) water model [35]. Force field parameters for THZ were obtained as follows. The initial THZ molecular geometry and atomic partial charges were obtained with Gaussian 03 [36] at the B3LYP/6-31G* level of theory. A preliminary model based on the modified, united-atom Gromos87 force field [37–39] was then constructed. A single THZ molecule in water was simulated in order to obtain typical conformations in an aqueous environment. Ten such conformations were randomly picked from the simulation trajectory, with their structures optimized and partial charges calculated with Gaussian at the HF/6-31G* level of theory. The final partial charge values (Supplementary Fig. 1) used in the membrane simulations was the averages over the ones obtained for the random conformations. All polar and aromatic hydrogen atoms were present explicitly in all simulated molecules. However, the hydrogen that determines the chirality is not present in our model of THZ molecule, since we use a united-atom force field. Therefore, our THZ molecule is not chiral. All parameters for THZ molecule are provided in Electronic Supplementary Material. Potassium or chloride ions with Gromos87 parameters were used as counterions to keep the systems electrostatically neutral. We used K+ instead of Na+ due to the latter's tendency to artificially order bilayers modeled by the Berger force field [40].

System construction

The pure POPC bilayer contains 64 lipids in each leaflet. To construct the mixed bilayer, 12 random POPC molecules in each leaflet were replaced by POPS molecules, and then 1 POPS molecule were added to each leaflet, to obtain 4:1 molar ratio. Both POPC and PCPS systems were pre-equilibrated and then production simulations were run for 167 and 250 ns, respectively. The initial rectangular boxes sizes were 64.215 Å × 64.215 Å × 114.14 Å for POPC,

Table 1 List of the performed simulations

Name	# drug molecules	Counterions	Simulation time (ns)	Time discarded for analysis (ns)	Bilayer composition
POPC	0	0	167	50	POPC
POPCTHZ16	16	16 Cl^-	153	50	POPC
POPCTHZ32	32	32 Cl^-	454	290	POPC
POPCTHZ64	64	64 Cl^-	1,200	1,200	POPC
PCPS	0	24 K^+	248	100	POPC/POPS
PCPSTHZ16	16	10 K^+	260	150	POPC/POPS
PCPSTHZ32	32	6 Cl^-	650	500	POPC/POPS
PCPSTHZ64	64	38 Cl^-	1,200	1,000	POPC/POPS

The POPC/POPS ratio in all simulations is 4:1

and 62.653 Å × 61.893 Å × 120.23 Å for PCPS. To construct the initial configurations of POPCTHZ16, POPCTHZ32, PCPSTHZ16 and PCPSTHZ32 systems, THZ molecules were placed in the aqueous phase uniformly, equidistant from each other. For construction of POPCTHZ64 and PCPSTHZ64 systems, all 64 molecules of THZ were not put in the aqueous phase initially, because THZ tends to micellize in the aqueous phase at such high concentrations [1]. Instead, 32 additional THZ molecules were added to the last frame of the POPCTHZ32 and PCPSTHZ32 simulations. The POPCTHZ64 system was studied with one additional simulation, where all 64 drug molecules had been placed inside the bilayer. All the details regarding the additional simulation were exactly the same as in the original POPCTHZ64 system.

Simulation procedure

All simulations were performed with GROMACS package version 3.3.3 [41]. Prior to the MD simulations, an energy minimization was performed using the steepest decent method with all bonds constrained. After successful energy minimization, that was indicated by the maximum force acting on the system being below 500 kJ mol^{-1} nm^{-1}, the systems were heated during 10 ps of MD by assigning random velocities to the particles according to a Maxwell distribution at 310 K. Other than the velocity generation, the parameters used for heating were identical to the parameters used for the production run. The leap-frog integrator [42] was used with a time step of 2 fs. The LINCS algorithm was used to constrain all bonds [43]. Periodic boundary conditions were applied in all three directions. A neighbor list with a 10 Å cut-off was used for non-bonded interactions and was updated every 10 steps. The van der Waals interactions were truncated with a cut-off of 10.0 Å. The 3-D particle mesh Ewald (PME) method with a 1.2 Å Fourier spacing and the interpolation order of 4 was employed for treatment of electrostatic interactions [44, 45]. The center of mass translation was removed at every step of the simulation. The simulated systems were maintained at the temperature of 310 K and the pressure of 1 bar according to the *NPT* statistical ensemble. Temperature coupling was performed using the Berendsen thermostat [46] separately for the solute (lipids and THZ molecules) and the solvent (counterions and water molecules). A semi-isotropic pressure coupling was applied using the Berendsen barostat [46], with a coupling constant of 0.1. The compressibility value for pure water, 4.5×10^{-5} bar^{-1}, was used. Trajectories were sampled every 10 ps. Ensemble averages were calculated only after all the THZ molecules partitioned into the bilayer. LPPs were obtained from the original trajectories using a modified version of GROMACS 4.0.2 [47] with the rerun option, employing the SHAKE algorithm for bond length constraints, a 1.8 nm cutoff for electrostatic interactions, and the Irving–Kirkwood contour [48]. More details about the LPP calculations using GROMACS can be found elsewhere [49, 50]. The POPCTHZ64 system has not been analyzed, because even after 1,200 ns of simulation, a significant number of THZ molecules remained in the aqueous phase in the form of micelles. The analysis was carried out using GROMACS programs and home-made scripts. Visualizations and snapshots were rendered using VMD [51].

Results

All simulations except POPCTHZ64 are stable and fully equilibrated, as indicated by the convergence of the potential energy and area per lipid profiles (data not shown) and the partitioning of THZ molecules inside the bilayers. The THZ molecule is considered partitioned when its center of mass is located below the lipid phosphate groups. Since THZ bears a positive charge, THZ interactions with negatively charged membrane are more pronounced. We will first describe the concentration-dependent partitioning of THZ, and its effects of THZ on lipid bilayers, followed by an atomic-scale description of the specific drug–lipid interactions. To some degree, the behavior of lipids in both membranes is similar, unless otherwise noted. Therefore, we present results mainly for the PCPS membrane. Complementary results for the POPC-only systems may be found in the Electronic Supplementary Material.

Partitioning of thioridazine in bilayers

Although THZ molecules incorporate into the lipid bilayer in all simulations, the timescale of partitioning differs significantly between in the different systems. Due to their amphiphilic nature, THZ molecules also tend to form micelles in water. The formation of micelles at higher concentrations of THZ slows down their insertion into the lipid bilayer. The insertion of THZ molecules in POPCTHZ16 takes up to 30 ns and up to 170 ns in POPCTHZ32. In the latter case, 13 THZ molecules cluster into a micelle that slowly incorporates into the membrane. In POPCTHZ64, 17 THZ molecules form an aggregate, which remains stable over the entire simulation time of 1,200 ns. Insertion of 16 THZ molecules into the PCPSTHZ16 bilayer takes 120 ns, and all 32 THZ molecules partition into PCPSTHZ32 after 180 ns. No micelles form in these systems. The significantly longer timescale of partitioning of the positively charged THZ into the negatively charged PCPS membrane, as compared to POPC, is counterintuitive. In PS-containing membranes, partitioned THZ

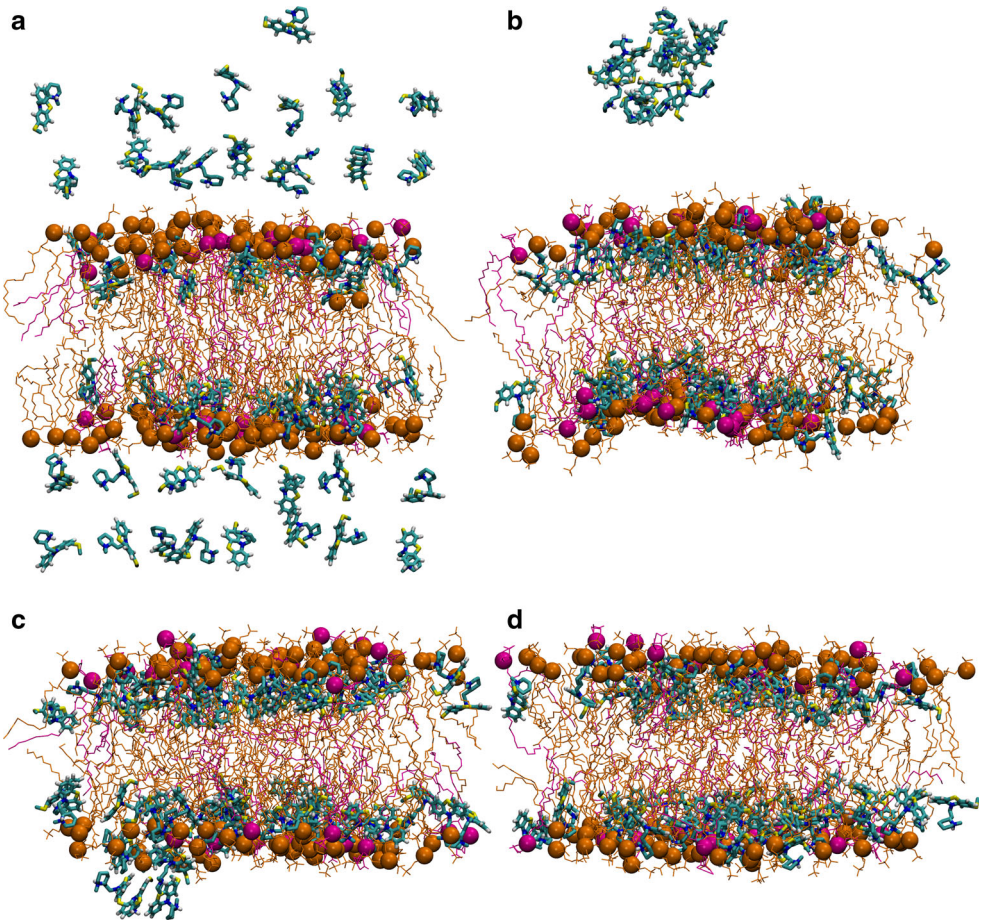

Fig. 2 Simulation snapshots from the PCPSTHZ64 simulation. POPC molecules are shown in *orange*, whereas POPS in *magenta*. POPC/POPS phosphate groups are shown as *orange*/*magenta spheres*, respectively. THZ is shown as *cyan* licorice, with its nitrogen atoms in *blue* and sulfur in *yellow*. Water is omitted for clarity. **a** 0 ns—initial structure, 32 THZ molecules are present in the membrane from the previous PCPS32 simulation and the other 32 molecules are added in the water phase. **b** 250 ns—most molecules partitioned into a membrane, while some of them assemble into a micelle. **c** 424 ns—partitioning of the micelle into the membrane. **d** 1,200 ns—final snapshot with all drug molecules located inside the membrane

molecules spend a longer time anchored at the lipid-water interface by means of electrostatic interactions between the negatively charged serine head group of POPS and the positively charged amine on THZ. The molecules eventually detach from the serine in PS, and anchor to the deeper-lying phosphate groups of POPC lipids (see later discussion on specific THZ–lipid interactions). In PCPSTHZ64, a small micelle of seven THZ molecules forms, which partitions into the membrane after 540 ns. Some representative snapshots from the PCPSTHZ64 simulation are shown in Fig. 2. In the additional POPCTHZ64 simulation, with all drug molecules initially placed in the bilayer, we do not observe any escape of THZ over 1,200 ns.

In both POPC and PCPS bilayers, positively charged THZ molecules are located near negatively charged phosphate groups and glycerol backbone of lipids (Fig. 3; Supplementary Fig. 2), corresponding to the Region II of the bilayer, i.e. the interface between the lipid tails and the headgroups, as defined by Marrink and Berendsen [52].

Density profiles further indicate (Supplementary Figs. 3–7) that the piperidine rings lie close to the lipid-water interface, while the aromatic phenothiazine moieties are buried more deeply in the bilayer. Concentration does

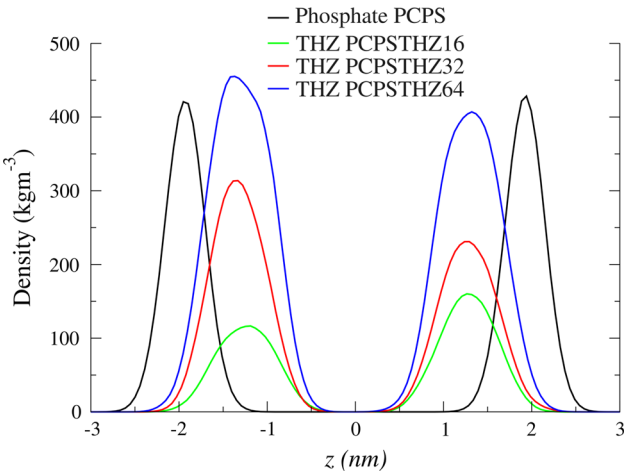

Fig. 3 Mass density profiles for the phosphate groups in PCPS system (*black curve*) and THZ molecules for different drug concentrations (16 drug molecules—*green curve*, 32—*red curve*, 64—*blue curve*) in the mixed bilayer simulations

not affect the location of THZ molecules in the bilayer. None of the THZs are found in the center of the bilayer, and we do not observe any flip-flop events in our

simulations. This means that the free energy barrier of crossing the membrane by the drug molecule is high.

To determine the orientation of THZ molecules in the lipid bilayer, we calculate the distributions of the angle between the plane of THZ aromatic rings and the bilayer normal (Supplementary Figs. 8, 9). The plane of the ring is spanned by the phenothiazine sulfur, nitrogen and carbon atom connected with a SCH_3 group. The angle is then equal to 90° minus the angle between the normal to this plane and the bilayer normal. The tilt angle distributions are quite broad, with the maxima placed around 90°, suggesting that THZ molecules adopt a variety of orientations inside the bilayer, and the perpendicular one, with respect to the bilayer normal, is preferred.

Effect of THZ on bilayer properties

The area per lipid and the thickness of both bilayers is provided in Table 2.

The projected area per lipid (A_L) was calculated by dividing the *xy* area of the simulation box by the number of lipids molecules in one monolayer. The bilayer thickness was obtained as the distance between phosphate groups in the two leaflets. A_L increases slightly by up to 3.5 % upon insertion of THZ into POPC in a concentration-dependent manner. We observe a similar behavior in the PCPS systems. However the insertion of 64 drug molecules causes a significant 15 % increase in A_L. The change in the membrane thickness is negligible in all systems containing 16 or 32 THZ molecules. However, in the PCPSTHZ64 system, the membrane thickness decreases by almost 7 %. The smaller area per lipid of the mixed PCPS bilayer than the area of the POPC bilayer is as consequence of the smaller head group of the cone-shaped POPS molecule [53].

The orientational order parameters of the hydrocarbon tails of the lipids are used to quantify the disorder of the membrane. The z-component of the order parameter for a given vector is defined by

$$S_z = \frac{3}{2}(\cos^2 \theta_z) - \frac{1}{2}$$

Table 2 Area per lipid and thickness (P–P distance)

Name	Area per lipid (Å^2)	Error (Å^2)	Thickness (nm)	Error (nm)
POPC	67.41	0.18	3.74	0.09
POPCTHZ16	67.97	0.37	3.77	0.08
POPCTHZ32	69.73	0.15	3.75	0.09
PCPS	65.90	0.16	3.83	0.08
PCPSTHZ16	65.99	0.16	3.87	0.09
PCPSTHZ32	67.13	0.24	3.87	0.09
PCPSTHZ64	76.09	0.15	3.61	0.08

where θ_z is the angle between the vector and the *z*-axis of the simulation box. The order parameters (*S*) of *sn*-1 acyl tails of POPC lipids are shown in Fig. 4.

For the pure bilayers, values of the order parameters are in agreement with previous simulation or experimental studies [54–56]. For the POPC membrane (Supplementary Fig. 10), THZ molecules order the lipid tails, and the effect is most pronounced near the interface, thus in the region of the bilayer where the drug is located. Insertion of 16 and 32 THZ molecules order lipid tails in the PCPS systems, similar to the POPC systems. However, insertion of 64 THZ molecules into PCPS not only slightly decreases the order parameters near the bilayer interface, compared to the PCPSTHZ32 system, but also significantly disorders lipids tails near the bilayer center. The significant area increase and thickness decrease correlate with the changes in order parameters. The incorporation of the drug molecules also induces significant changes in the LPPs of the bilayers (Fig. 5).

The LPP $p_L(z)$ along the bilayer normal is defined as

$$p_L(z) = \frac{p_{xx}(z) + p_{yy}(z)}{2} - p_{zz}(z)$$

where p_{xx}, p_{yy} and p_{zz} are elements of the pressure tensor for a given *z*. The regions most significantly altered by THZ are the highly negative peaks located approximately 2 nm away from the bilayer center, referred to the interfacial tensile (negative) pressure region [57, 58]. The position of these peaks coincides with the region occupied by the drug molecules, and the presence of THZ leads to the elevated pressure (decreased tension) by at least a few hundred bars.

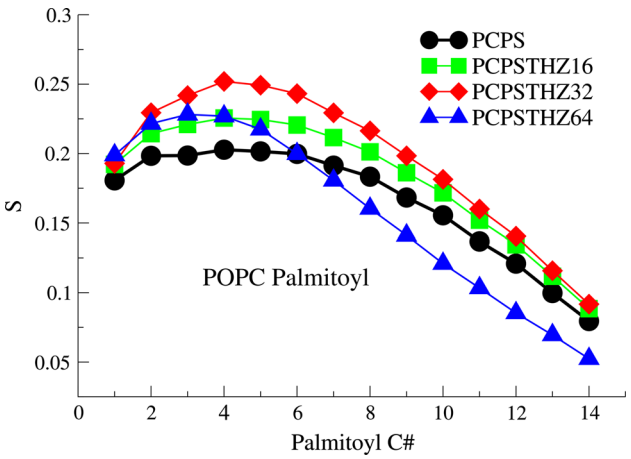

Fig. 4 Lipid tails order parameters for the POPC palmitoyl tails in the mixed bilayer simulations. The trend is similar for the POPS acyl tails (data not shown) and for the POPC tails in the POPC membrane (Supplementary Fig. 10). THZ orders lipid tails near the bilayer interface in PCPSTHZ16 and PCPSTHZ32 and disorders them significantly near the bilayer center in PCPSTHZ64

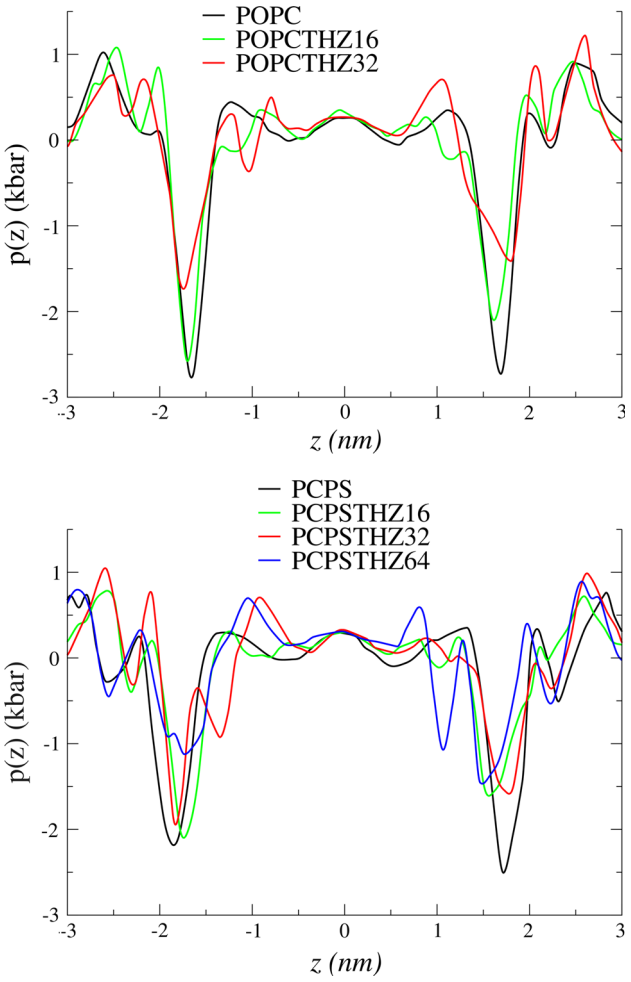

Fig. 5 Lateral pressure profiles. The position of the two altered peaks, ~2 nm from the bilayer center, coincides with the location of THZ inside the membrane. The incorporation of the drug decreases the interfacial tensile pressure, up to 1 kbar in PCPS64 systems

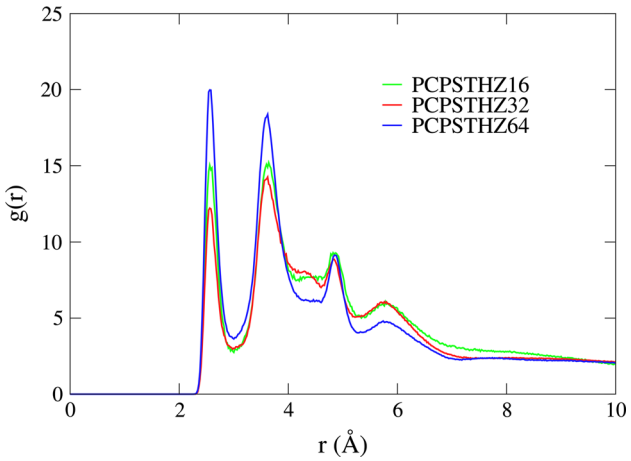

Fig. 6 Radial distribution functions between the POPC lipid phosphate groups and amino groups of THZ in the different PCPS systems. THZ forms salt bridges with the lipid phosphate moiety

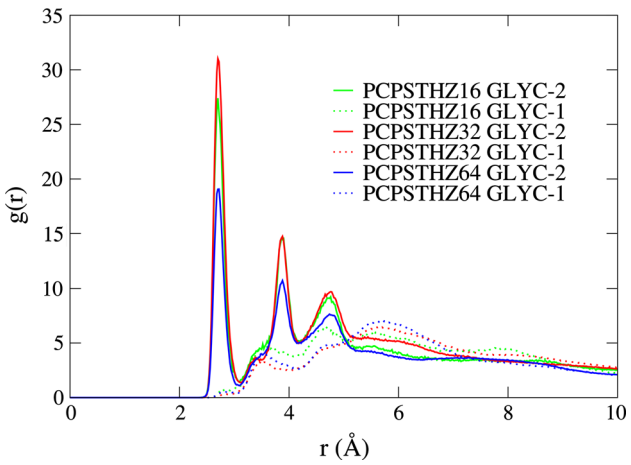

Fig. 7 Radial distribution functions between POPC glycerol regions—GLYC-1 (*sn*-1 tails) and GLYC-2 (*sn*-2 tails) and amino groups of THZ in the different PCPS systems. THZ interacts with the GLYC-2 region of POPC

Specific thioridazine–lipid interactions

Density profiles (data not shown) and the visual inspection suggest that the positively charged protonated amino group of THZ's piperidine ring interacts with both the lipid headgroup and the glycerol backbone region via electrostatic interactions and/or hydrogen bonds (salt bridges). Hydrogen bonds are identified using the criteria of distance of 3.5 Å between the donor (D) and the acceptor (A), and the HDA angle to be no more than 30°. THZ molecules interact with POPC phosphate groups (Fig. 6), irrespective of the drug concentration used.

However, these interactions are significantly weaker with POPS lipids (Supplementary Fig. 11). The POPS serine ammonium group forms an intra-molecular hydrogen bond with its own phosphate group [55]. The POPS phosphate group is thus sterically confined and also less available for intermolecular hydrogen bonding and electrostatic interactions. We observe the exact same situation in our simulations of systems containing POPS lipids. POPS does not form an inter-molecular hydrogen bond with a phosphate group of POPC, as its own phosphate group is closer than the phosphate of another molecule. Interestingly, the amino group of THZ interacts almost exclusively with the *sn*-2 glycerol group (Fig. 7; Supplementary Fig. 12) of lipids, and not with their *sn*-1 backbone.

Cholesterol and ergosterol also bind preferentially to the *sn*-2 glycerol group of lipids [59]. Such a preference of a hydrophilic group (–OH in sterols and NH_3^+ in THZ) for the *sn*-2 backbone is ascribed to the increased hydration

level of the *sn*-2 backbone that enables the preferential interactions of water with the sterols hydroxyl group, similar to the THZ amino moiety.

Discussion

In this study, we use atomistic long-scale MD simulations to investigate interactions of ex-psychotic, potent anti-TB and anticancer drug, THZ, with two types of model lipid bilayers constituted of POPC and a mixture of POPC and POPS lipids. The latter, which contains negatively charged lipids, may be viewed as a simplistic model of bacterial, cancer cell, and also synaptic membrane [60–62], while the former may serve as the simplest model of the typical, zwitterionic, mammalian cell membrane [63]. We consider only the cationic version of the drug, as this form is more likely in the neutral environment. However, due to the high value of THZ distribution coefficient (log D = 4.66) [31] THZ may be present in membranes in its neutral form, particularly in uncharged membranes. The neutral form of THZ may be of importance for drug delivery, as it might cross bilayers more easily, while the effect on membranes might be ascribed to the charged version of the drug [30].

The concentration at which THZ has a significant effect on bilayer properties in our simulations seems much higher compared to the obtainable limit in human plasma (0.5–1 μg mL^{-1}) [15]. So how clinically relevant are the concentrations used in this study? We cannot envisage of a straightforward way to relate blood plasma levels of the drug to their concentration in a nanometer-sized membrane patch, because first, THZ is known to accumulate at high concentrations in certain tissues, and second, it is certainly possible that such concentrations in the bilayer might locally exist, due to the membrane compartmentalization and formation of PS-enriched dynamic domains [64, 65]. In any case, it is impossible to judge if the concentrations used in our simulations reflect clinical concentrations, because we simulate only a small bilayer patch that is enriched with THZ. The conundrum will be best answered when the actual concentration of THZ in tissue membranes is experimentally measured. Nevertheless, our studies provide a unique insight into membrane–THZ interactions on the atomistic scale and reveals that the drug impact on the membrane properties may vary significantly depending on the local drug concentration occurring in the membrane. Our simulations clearly show that THZ can accumulate at very high concentrations in membranes of specific composition. The fact that THZ interacts and perturbs lipid bilayers, which are omnipresent in various tissues, is in line with the wide pharmacological profile of THZ. Furthermore, THZ accumulates more in anionic membranes, which also suggests that it might preferentially target bacterial membranes.

THZ molecules partition into both POPC and PCPS membranes. The highest concentration (drug:lipid ratio 1:2) inside the membrane is obtained only for the mixed bilayer, due to the additional driving force arising from the negative charge of the POPC/POPS bilayer. Partitioning time courses vary considerably between systems, and 540 ns is the longest time. Such long timescales are caused by the tendency of THZ molecules to form micelle-like aggregates in the water phase, and cannot be predicted from free energy profiles along the bilayer alone. The kinetics of THZ incorporation depends also on the initial conditions: in the systems with high THZ concentration: POPCTHZ64 and PCPSTHZ64, we tried to accelerate the partitioning by placing 32 drug molecules in the bilayer, and the remaining 32 in the water phase, to decrease the likelihood of self-assembly and micelle formation. This approach results in partitioning of all THZ molecules in the PCPSTHZ64 system, albeit slowly (540 ns), whereas for the POPCTHZ64 even 1,200 ns was not sufficient for the full partitioning. The THZ aggregates in water consist of 7–17 molecules, which is in agreement with experimental data of phenothiazines that have the aggregation number N of the order of 6–15 [1]. The amphiphilic character of THZ arises from its structural properties—the protonated amino group is highly hydrophilic while the aromatic tricyclic backbone exhibits a bulk hydrophobic behavior. Therefore, THZ molecules are present in the interfacial region of the membrane, similar to small cyclic terpenes [66], or anesthetics, such as propofol [10] and ketamine [50]. This location is typical for charged aromatic molecules studied by MD simulations [10], fluorescence spectroscopy and NMR measurements [67–69]. However, the preferential orientation of the molecule with the phenothiazine ring placed almost perpendicularly to the bilayer normal is somewhat surprising. The flat rings of indole and pyrene align parallel to the lipid tails [70]. Such an orientation is also typical for rings of cholesterol [71]. In case of THZ, the aromatic rings are connected with a piperidine ring via a linker of two methylene groups. Therefore, the phenothiazine group may be viewed as a molecular 'anchor' linked to the small functional group. As the piperidine ring interacts strongly with the lipid phosphate group and glycerol backbone, it biases the conformational space of the pendant aromatic tricycle, making the parallel alignment of the rings highly unfavorable. Such complex behavior underlines the fact that the behavior of complex molecules with few functional groups inside bilayers might be difficult to predict by a simple analysis of their chemical composition. Additionally, such an orientation of the bulky, planar group near lipid acyl chains should not increase their order parameters.

The bilayer structure is retained in every system, even at a high 1:2 drug:lipid ratio. THZ molecules are spread evenly in the bilayer and do not form clusters after partitioning. The average cross-sectional area per lipid increases upon addition of the drug in every system, but the membrane thickness hardly changes at moderate drug concentration (drug:lipid ratio 1:8 and 1:4). These changes are therefore attributed to the occupation of the interfacial free volume by THZ molecules. On the contrary, in the PCPSTHZ64 system, the membrane thickness is significantly reduced, below the value of the pure membrane, accompanied by the significant expansion of the bilayer in the *xy*-plane, as indicated by a sharp increase of the area per lipid at the highest drug:lipid ratio. Note that THZ molecules have not been considered in area per lipid calculations, therefore its value cannot be viewed as an area occupied by a single lipid molecule, especially due to the high number of THZ in membranes. Edholm and Nagle proposed a canonical way of deriving the area occupied by each molecule in binary bilayers, the so-called partial-specific area [72]. However, the main strength of this approach lies in an ability to predict the area of both molecular species that constitute the membrane, as a function of their molecular fraction. This is particularly important for native membrane components, e.g. different phospholipids or sterols, as it might indicate the ideal and non-ideal mixing of both species [73]. In the current report, the simple definition of area per lipid is a good indicator of the bilayer lateral structure and it suggests the existence of a certain threshold of drug molecules that the membrane can accumulate without significant structural reorganization. Above this point, membrane properties are altered differently than before. In line with the above hypothesis, 16 and 32 THZ molecules order the lipid chains near the glycerol backbone and the THZ piperidine rings, while the presence of 64 molecules leads to the membrane disordering, especially closer to the bilayer center. After the lateral expansion of the bilayer, the lipid tails are able to probe more free volume, which leads to their higher mobility i.e. elevated level of the molecular disorder. It is also not easy to relate this behavior to the previous MD simulations of similar, small molecules containing aromatic groups. We have recently reviewed current literature regarding MD simulations of such compounds, e.g. non-steroidal anti-inflammatory drugs (NSAIDs) and local anesthetics, with lipid membranes [10]. Usually, charged versions of these drugs slightly disorder membranes, and their aromatic rings do not cause any measurable ordering effect. The observed disruption of the membrane structure is then annotated to the charged group interacting with glycerol and phosphate groups. However, THZ's amino group is a part of a six-membered, heterocylic ring that, due to its bulky nature, orders membranes at lower concentrations. These findings are in line with experimental studies, which reported the solidification effect of phenothiazines on the lipid membranes, at concentrations lower than used in the current study [74]. In the system with the highest THZ concentration, a sharp decrease of the order parameters is observed. To the best of our knowledge, the reverse effect on the order parameters caused by the same molecule, only in a higher concentration, is reported for the first time. It is also worth mentioning that cholesterol decreases the partitioning coefficient of phenothiazines in lipid bilayers [20]. Together with the elevated propensity of THZ toward negatively charged lipids demonstrated in this study, this provides a putative explanation of THZ selectively targeting for cancer cells, whose membranes may be richer in anionic lipids [61, 75].

The presence of THZ molecules in bilayers also alters their lateral pressure profiles, which again is the most visible in the highest drug concentration (PCPSTHZ64 system). The observed decrease of the tensile pressure between lipid headgroups supports the hypothesis, that small molecules may significantly rebalance the membrane lateral pressure [76]. The overall shape of profiles obtained from MD simulations, e.g. the ones calculated for the anesthetic ketamine [50], is reproduced. However, in case of THZ the changes are much more visible, arising from higher concentrations used in this study. Also note that we did not artificially average the profiles over two membrane leaflets, therefore the profiles look more distorted, due to the non-even distribution of THZ between the leaflets. The impact of such a shift of the LPP in the membrane can be gauged from the force such a pressure change might exert on a trans-membrane protein. The pressure difference in the membrane interfacial region between PCPS and PCPS64 systems is $\sim$1,000 bars. Simple calculations suggest that such a pressure shift exerts a force of $\sim$130 pN on a thin strip of height 0.1 nm on the surface of the trans-membrane cylindrical protein of 2 nm radius, with the corresponding energy of $\sim 6\ k_bT$ when considering 0.2 nm displacement of the protein against the pressure [77]. Six k_bT is comparable to the free energy of conformational changes in integral proteins [78], such as drug efflux pumps, which THZ has been hypothesized to inhibit. The changes in lateral pressure profile therefore do not rule out a membrane-mediated inhibition of drug-efflux pumps by THZ. Nevertheless, the experimental evaluation of the lateral pressure in membranes is still extremely difficult and we remain cautious when interpreting changes in LPP observed in simulations.

Conclusions

We show that the neuroleptic drug with antimicrobial and anticancer activity, THZ, interacts strongly with lipid

membranes and significantly alters their properties. In agreement with the lipophilic character of THZ, we show that THZ is able to accumulate in lipid membranes, and such accumulation occurs to a higher degree in the presence of negatively charged lipids, which are present in higher concentrations in cancerous cells and bacteria. Membrane properties upon THZ insertion are altered significantly enough to potentially alter the conformational equilibria of proteins such as drug efflux pumps. THZ does not disrupt bilayers even at very high concentrations, but does cause significant membrane thinning. Our results reinforce the hypothesis of the membrane-mediated mechanism of action of phenothiazines in general, and show that THZ ability of concentrating in some cells membrane are, at least partially, electrostatically driven, and may even induce conformational transitions of trans-membrane proteins. However further computational and experimental studies, with more complex, cholesterol-containing membranes are required to fully characterize the membrane-mediated mechanism of action of phenothiazines. We believe further research into the mechanism of action is warranted by the tremendous potential of THZ as an inexpensive anti-TB drug and as a possible anti-cancer agent as well.

Acknowledgments MEMPHYS - Center for Biomembrane Physics is supported by the Danish National Research Foundation. The computations were done at the SDU node of the Danish Center for Scientific Computing (DCSC). Himanshu Khandelia is funded by a Lundbeck Junior Group Leader Investigator Fellowship. We thank Emppu Salonen for the QM/MM calculations and the parametrization of THZ molecule. We also thank Jette Kristiansen for helpful discussions.

References

1. Schreier S, Malheiros SV, de Paula E (2000) Surface active drugs: self-association and interaction with membranes and surfactants. Physicochemical and biological aspects. Biochim Biophys Acta 1508(1–2):210–234
2. Imming P, Sinning C, Meyer A (2006) Drugs, their targets and the nature and number of drug targets. Nat Rev Drug Discov 5(10):821–834
3. Hendrich AB, Michalak K (2003) Lipids as a target for drugs modulating multidrug resistance of cancer cells. Curr Drug Targets 4(1):23–30
4. Khandelia H, Ipsen JH, Mouritsen OG (2008) The impact of peptides on lipid membranes. Biochim Biophys Acta Biomembr 1778(7–8):1528–1536
5. Jutila A, Söderlund T, Pakkanen AL, Huttunen M, Kinnunen PKJ (2001) Comparison of the effects of clozapine, chlorpromazine, and haloperidol on membrane lateral heterogeneity. Chem Phys Lipids 112(2):151–163
6. Killian JA (1998) Hydrophobic mismatch between proteins and lipids in membranes. Biochim Biophys Acta Rev Biomembr 1376(3):401–415
7. Jensen MØ, Mouritsen OG (2004) Lipids do influence protein function—the hydrophobic matching hypothesis revisited. Biochim Biophys Acta Biomembr 1666(1–2):205–226
8. Cantor RS (1997) The lateral pressure profile in membranes: a physical mechanism of general anesthesia. Biochemistry 36(9):2339–2344
9. Cantor RS (1997) Lateral pressures in cell membranes: a mechanism for modulation of protein function. J Phys Chem B 101(10):1723–1725
10. Kopec W, Telenius J, Khandelia H (2013) Molecular dynamics simulations of the interactions of medicinal plant extracts and drugs with lipid bilayer membranes. FEBS J. doi:10.1111/febs.12286
11. Seeger HM, Gudmundsson ML, Heimburg T (2007) How anesthetics, neurotransmitters, and antibiotics influence the relaxation processes in lipid membranes. J Phys Chem B 111(49):13858–13866
12. Scheidt HA, Huster D (2008) The interaction of small molecules with phospholipid membranes studied by 1H NOESY NMR under magic-angle spinning. Acta Pharmacol Sin 29(1):35–49
13. Barry J, Fritz M, Brender JR, Smith PES, Lee D-K, Ramamoorthy A (2009) Determining the effects of lipophilic drugs on membrane structure by solid-state NMR spectroscopy: the case of the antioxidant curcumin. J Am Chem Soc 131(12):4490–4498. doi:10.1021/ja809217u
14. Klitgaard JK, Skov MN, Kallipolitis BH, Kolmos HJ (2008) Reversal of methicillin resistance in *Staphylococcus aureus* by thioridazine. J Antimicrob Chemother 62(6):1215–1221
15. Thanacoody HK (2007) Thioridazine: resurrection as an antimicrobial agent? Br J Clin Pharmacol 64(5):566–574. doi:10.1111/j.1365-2125.2007.03021.x
16. Abbate E, Vescovo M, Natiello M, Cufre M, Garcia A, Gonzalez Montaner P, Ambroggi M, Ritacco V, van Soolingen D (2012) Successful alternative treatment of extensively drug-resistant tuberculosis in Argentina with a combination of linezolid, moxifloxacin and thioridazine. J Antimicrob Chemother 67(2):473–477. doi:10.1093/jac/dkr500
17. Lialiaris T, Pantazaki A, Sivridis E, Mourelatos D (1992) Chlorpromazine-induced damage on nucleic acids: a combined cytogenetic and biochemical study. Mutat Res Fundam Mol Mech Mutagen 265(2):155–163
18. Sharma S, Singh A (2011) Phenothiazines as anti-tubercular agents: mechanistic insights and clinical implications. Expert Opin Invest Drugs 20(12):1665–1676
19. Salih FA, Kaushik NK, Sharma P, Choudary GV, Murthy PS, Venkitasubramanian TA (1991) Calmodulin-like activity in mycobacteria. Indian J Biochem Biophys 28(5–6):491–495
20. Michalak K, Wesolowska O, Motohashi N, Molnar J, Hendrich AB (2006) Interactions of phenothiazines with lipid bilayer and their role in multidrug resistance reversal. Curr Drug Targets 7(9):1095–1105
21. Langerman L, Bansinath M, Grant GJ (1994) The partition coefficient as a predictor of local anesthetic potency for spinal anesthesia: evaluation of five local anesthetics in a mouse model. Anesth Analg 79(3):490–494
22. Forrest FM, Forrest IS, Roizin L (1963) Clinical, biochemical and post mortem studies on a patient treated with chlorpromazine. Agressologie 4:259–265
23. Sachlos E, Risueno RM, Laronde S, Shapovalova Z, Lee JH, Russell J, Malig M, McNicol JD, Fiebig-Comyn A, Graham M, Levadoux-Martin M, Lee JB, Giacomelli AO, Hassell JA, Fischer-Russell D, Trus MR, Foley R, Leber B, Xenocostas A, Brown ED, Collins TJ, Bhatia M (2012) Identification of drugs including a dopamine receptor antagonist that selectively target cancer stem cells. Cell 149(6):1284–1297. doi:10.1016/j.cell.2012.03.049
24. Seeman P, Lee T (1975) Antipsychotic drugs: direct correlation between clinical potency and presynaptic action on dopamine neurons. Science 188(4194):1217–1219

25. Carlo RD, Muccioli G, Bellussi G, Portaleone P, Ghi P, Racca S, Carlo FD (1986) Steroid, prolactin, and dopamine receptors in normal and pathologic breast tissue. Ann NY Acad Sci 464(1):559–562. doi:10.1111/j.1749-6632.1986.tb16068.x
26. Peters GH, Wang C, Cruys-Bagger N, Velardez GF, Madsen JJ, Westh P (2013) Binding of serotonin to lipid membranes. J Am Chem Soc 135(6):2164–2171. doi:10.1021/ja306681d
27. Jodko-Piorecka K, Litwinienko G (2013) First experimental evidence of dopamine interactions with negatively charged model biomembranes. ACS Chem Neurosci. doi:10.1021/cn4000633
28. Orlowski A, Grzybek M, Bunker A, Pasenkiewicz-Gierula M, Vattulainen I, Mannisto PT, Rog T (2012) Strong preferences of dopamine and l-dopa towards lipid head group: importance of lipid composition and implication for neurotransmitter metabolism. J Neurochem 122(4):681–690. doi:10.1111/j.1471-4159.2012.07813.x
29. Amaral L, Kristiansen JE, Viveiros M, Atouguia J (2001) Activity of phenothiazines against antibiotic-resistant *Mycobacterium tuberculosis*: a review supporting further studies that may elucidate the potential use of thioridazine as anti-tuberculosis therapy. J Antimicrob Chemother 47(5):505–511
30. Castaing M, Brouant P, Loiseau A, Santelli-Rouvier C, Santelli M, Alibert-Franco S, Mahamoud A, Barbe J (2000) Membrane permeation by multidrug-resistance-modulators and non-modulators: effects of hydrophobicity and electric charge. J Pharm Pharmacol 52(3):289–296
31. Gulyaeva N, Zaslavsky A, Lechner P, Chlenov M, McConnell O, Chait A, Kipnis V, Zaslavsky B (2003) Relative hydrophobicity and lipophilicity of drugs measured by aqueous two-phase partitioning, octanol-buffer partitioning and HPLC. A simple model for predicting blood-brain distribution. Eur J Med Chem 38(4):391–396
32. Christensen JB, Hendricks O, Chaki S, Mukherjee S, Das A, Pal TK, Dastidar SG, Kristiansen JE (2013) A comparative analysis of in vitro and in vivo efficacies of the enantiomers of thioridazine and its racemate. PLoS One 8(3):e57493. doi:10.1371/journal.pone.0057493
33. Berger O, Edholm O, Jahnig F (1997) Molecular dynamics simulations of a fluid bilayer of dipalmitoylphosphatidylcholine at full hydration, constant pressure, and constant temperature. Biophys J 72(5):2002–2013. doi:10.1016/s0006-3495(97)78845-3
34. Bachar M, Brunelle P, Tieleman DP, Rauk A (2004) Molecular dynamics simulation of a polyunsaturated lipid bilayer susceptible to lipid peroxidation. J Phys Chem B 108(22):7170–7179. doi:10.1021/Jp036981u
35. Berendsen HJC, Postma JPM, van Gunsteren WF, Hermans J (1981) Interaction models for water in relation to protein hydration. Intermolecular Forces 14:331–342
36. Frisch MJ, Trucks GW, Schlegel HB, Scuseria GE, Robb MA, Cheeseman JR, Montgomery JA Jr, Vreven T, Kudin KN, Burant JC, Millam JM, Iyengar SS, Tomasi J, Barone V, Mennucci B, Cossi M, Scalmani G, Rega N, Petersson GA, Nakatsuji H, Hada M, Ehara M, Toyota K, Fukuda R, Hasegawa J, Ishida M, Nakajima T, Honda Y, Kitao O, Nakai H, Klene M, Li X, Knox JE, Hratchian HP, Cross JB, Bakken V, Adamo C, Jaramillo J, Gomperts R, Stratmann RE, Yazyev O, Austin AJ, Cammi R, Pomelli C, Ochterski JW, Ayala PY, Morokuma K, Voth GA, Salvador P, Dannenberg JJ, Zakrzewski VG, Dapprich S, Daniels AD, Strain MC, Farkas O, Malick DK, Rabuck AD, Raghavachari K, Foresman JB, Ortiz JV, Cui Q, Baboul AG, Clifford S, Cioslowski J, Stefanov BB, Liu G, Liashenko A, Piskorz P, Komaromi I, Martin RL, Fox DJ, Keith T, Laham A, Peng CY, Nanayakkara A, Challacombe M, Gill PMW, Johnson B, Chen W, Wong MW, Gonzalez C, Pople JA (2004) Gaussian 03. Gaussian, Inc., Wallingford, CT
37. Van Gunsteren WF, Berendsen HJC (1987) Groningen molecular simulation (GROMOS). Library manual, Biomos, Groningen, The Netherlands, p 1–221
38. van Buuren AR, Marrink SJ, Berendsen HJC (1993) A molecular dynamics study of the decane/water interface. J Phys Chem 97(36):9206–9212. doi:10.1021/j100138a023
39. Mark AE, van Helden SP, Smith PE, Janssen LHM, van Gunsteren WF (1994) Convergence properties of free energy calculations: alpha.-cyclodextrin complexes as a case study. J Am Chem Soc 116(14):6293–6302. doi:10.1021/ja00093a032
40. Khandelia H, Witzke S, Mouritsen OG (2010) Interaction of salicylate and a terpenoid plant extract with model membranes: reconciling experiments and simulations. Biophys J 99(12):3887–3894. doi:10.1016/j.bpj.2010.11.009
41. Lindahl E, Hess B, van der Spoel D (2001) GROMACS 3.0: a package for molecular simulation and trajectory analysis. J Mol Model 7(8):306–317
42. Leach AR (2001) Molecular modeling principles and applications, 2nd edn. Pearson Education Limited, p 356
43. Hess B (2008) P-LINCS: a parallel linear constraint solver for molecular simulation. J Chem Theory Comput 4(1):116–122
44. Darden T, York D, Pedersen L (1993) Particle mesh Ewald: an N·log(N) method for Ewald sums in large systems. J Chem Phys 98(12):10089–10092
45. Essmann U, Perera L, Berkowitz ML, Darden T, Lee H, Pedersen LG (1995) A smooth particle mesh Ewald method. J Chem Phys 103(19):8577–8593
46. Berendsen HJC, Postma JPM, Van Gunsteren WF, Dinola A, Haak JR (1984) Molecular dynamics with coupling to an external bath. J Chem Phys 81(8):3684–3690
47. Lindahl E, Edholm O (2000) Spatial and energetic–entropic decomposition of surface tension in lipid bilayers from molecular dynamics simulations. J Chem Phys 113(9):3882–3893
48. Irving JH, Kirkwood JG (1950) The statistical mechanical theory of transport processes. IV. The equations of hydrodynamics. J Chem Phys 18(6):817–829
49. Terama E, Ollila OHS, Salonen E, Rowat AC, Trandum C, Westh P, Patra M, Karttunen M, Vattulainen I (2008) Influence of ethanol on lipid membranes: from lateral pressure profiles to dynamics and partitioning. J Phys Chem B 112(13):4131–4139
50. Jerabek H, Pabst G, Rappolt M, Stockner T (2010) Membrane-mediated effect on ion channels induced by the anesthetic drug ketamine. J Am Chem Soc 132(23):7990–7997. doi:10.1021/ja910843d
51. Humphrey W, Dalke A, Schulten K (1996) VMD: visual molecular dynamics. J Mol Graph 14(1):33–38
52. Marrink SJ, Berendsen HJC (1996) Permeation process of small molecules across lipid membranes studied by molecular dynamics simulations. J Phys Chem 100(41):16729–16738
53. Pautot S, Frisken BJ, Weitz DA (2003) Engineering asymmetric vesicles. Proc Natl Acad Sci USA 100(19):10718–10721. doi:10.1073/pnas.1931005100
54. Abu-Baker S, Qi X, Lorigan GA (2007) Investigating the interaction of Saposin C with POPS and POPC phospholipids: a solid-state NMR spectroscopic study. Biophys J 93(10):3480–3490
55. Mukhopadhyay P, Monticelli L, Tieleman DP (2004) Molecular dynamics simulation of a palmitoyl-oleoyl phosphatidylserine bilayer with Na+ counterions and NaCl. Biophys J 86(3):1601–1609
56. Ferreira TM, Coreta-Gomes F, Samuli Ollila OH, Moreno MJ, Vaz WLC, Topgaard D (2013) Cholesterol and POPC segmental order parameters in lipid membranes: solid state 1H–13C NMR and MD simulation studies. Phys Chem Chem Phys 15(6):1976–1989
57. Bagatolli LA, Ipsen JH, Simonsen AC, Mouritsen OG (2010) An outlook on organization of lipids in membranes: searching for a realistic connection with the organization of biological membranes. Prog Lipid Res 49(4):378–389

58. Bagatolli LA, Mouritsen OG (2013) Is the fluid mosaic (and the accompanying raft hypothesis) a suitable model to describe fundamental features of biological membranes? What may be missing? Front Plant Sci 4:457. doi:10.3389/fpls.2013.00457
59. Cournia Z, Ullmann GM, Smith JC (2007) Differential effects of cholesterol, ergosterol and lanosterol on a dipalmitoyl phosphatidylcholine membrane: a molecular dynamics simulation study. J Phys Chem B 111(7):1786–1801
60. Epand RM, Epand RF (2011) Bacterial membrane lipids in the action of antimicrobial agents. J Pept Sci 17(5):298–305. doi:10.1002/psc.1319
61. Riedl S, Rinner B, Asslaber M, Schaider H, Walzer S, Novak A, Lohner K, Zweytick D (2011) In search of a novel target—phosphatidylserine exposed by non-apoptotic tumor cells and metastases of malignancies with poor treatment efficacy. Biochim Biophys Acta 1808(11):2638–2645. doi:10.1016/j.bbamem.2011.07.026
62. Milutinovic PS, Yang L, Cantor RS, Eger EI II, Sonner JM (2007) Anesthetic-like modulation of a gamma-aminobutyric acid type A, strychnine-sensitive glycine, and N-methyl-d-aspartate receptors by coreleased neurotransmitters. Anesth Analg 105(2):386–392. doi:10.1213/01.ane.0000267258.17197.7d
63. van Meer G, Voelker DR, Feigenson GW (2008) Membrane lipids: where they are and how they behave. Nat Rev Mol Cell Biol 9(2):112–124. doi:10.1038/nrm2330
64. Denisov G, Wanaski S, Luan P, Glaser M, McLaughlin S (1998) Binding of basic peptides to membranes produces lateral domains enriched in the acidic lipids phosphatidylserine and phosphatidylinositol 4,5-bisphosphate: an electrostatic model and experimental results. Biophys J 74(2 Pt 1):731–744. doi:10.1016/s0006-3495(98)73998-0
65. Leventis PA, Grinstein S (2010) The distribution and function of phosphatidylserine in cellular membranes. Annu Rev Biophys 39:407–427. doi:10.1146/annurev.biophys.093008.131234
66. Witzke S, Duelund L, Kongsted J, Petersen M, Mouritsen OG, Khandelia H (2010) Inclusion of terpenoid plant extracts in lipid bilayers investigated by molecular dynamics simulations. J Phys Chem B 114(48):15825–15831
67. Frenzel J, Arnold K, Nuhn P (1978) Calorimetric, 13C NMR, and 31P NMR studies on the interaction of some phenothiazine derivatives with dipalmitoyl phosphatidylcholine model membranes. Biochim Biophys Acta Biomembr 507(2):185–197
68. Lichtenberger LM, Zhou Y, Jayaraman V, Doyen JR, O'Neil RG, Dial EJ, Volk DE, Gorenstein DG, Boggara MB, Krishnamoorti R (2012) Insight into NSAID-induced membrane alterations, pathogenesis and therapeutics: characterization of interaction of NSAIDs with phosphatidylcholine. Biochim Biophys Acta 1821(7):994–1002. doi:10.1016/j.bbalip.2012.04.002
69. Parry MJ, Alakoskela JMI, Khandelia H, Kumar SA, Jäättelä M, Mahalka AK, Kinnunen PKJ (2008) High-affinity small molecule-phospholipid complex formation: binding of siramesine to phosphatidic acid. J Am Chem Soc 130(39):12953–12960
70. MacCallum JL, Tieleman DP (2008) Interactions between small molecules and lipid bilayers. Curr Top Membr 60:227–256. doi:10.1016/S1063-5823(08)00008-2
71. Rog T, Pasenkiewicz-Gierula M, Vattulainen I, Karttunen M (2009) Ordering effects of cholesterol and its analogues. Biochim Biophys Acta 1788(1):97–121. doi:10.1016/j.bbamem.2008.08.022
72. Edholm O, Nagle JF (2005) Areas of molecules in membranes consisting of mixtures. Biophys J 89(3):1827–1832. doi:10.1529/biophysj.105.064329
73. Hermetter A, Kopec W, Khandelia H (2013) Conformations of double-headed, triple-tailed phospholipid oxidation lipid products in model membranes. Biochim Biophys Acta 1828:1700–1706. doi:10.1016/j.bbamem.2013.03.030
74. Hendrich AB, Wesołowska O, Komorowska M, Motohashi N, Michalak K (2002) The alterations of lipid bilayer fluidity induced by newly synthesized phenothiazine derivative. Biophys Chem 98(3):275–285
75. Dobrzynska I, Szachowicz-Petelska B, Sulkowski S, Figaszewski Z (2005) Changes in electric charge and phospholipids composition in human colorectal cancer cells. Mol Cell Biochem 276(1–2):113–119. doi:10.1007/s11010-005-3557-3
76. Cantor RS (2003) Receptor desensitization by neurotransmitters in membranes: are neurotransmitters the endogenous anesthetics? Biochemistry 42(41):11891–11897
77. Samuli Ollila OH, Rog T, Karttunen M, Vattulainen I (2007) Role of sterol type on lateral pressure profiles of lipid membranes affecting membrane protein functionality: comparison between cholesterol, desmosterol, 7-dehydrocholesterol and ketosterol. J Struct Biol 159(2):311–323. doi:10.1016/j.jsb.2007.01.012
78. Lau AY, Roux B (2007) The free energy landscapes governing conformational changes in a glutamate receptor ligand-binding domain. Structure 15(10):1203–1214. doi:10.1016/j.str.2007.07.015